Journal of Engineering Technology
Volume 6, Issue 2, July. 2018, PP. 1-12
RESEARCH ARTICLE -ENGINEERNG TECHNOLOGY

A nonlinear model of a reverse osmosis desalination system: experimental validation

Abderrahmen Ben Chaabene[1,3*], Khira Ouelhazi[1], Imene Chellouf[2], Mohamed Said Chahri[3], Anis Sellami[1]

[1]Industrial Systems Engineering and Renewable Energies-Laboratory, Higher National School of Engineers of Tunis (ENSIT), Tunisia
[2]Electrical Engineering Department, High Institute of Technology Educations of Nabeul
[3]Electronic Department, Technical College of Abha, TVTC, KSA

Abstract: Nowadays, desalination has become a very affordable solution to provide drinking water. Reverse Osmosis (RO) desalination systems are the most widely used processes for desalting brackish or sea water. In order to operate these plants at their optimum conditions, an efficient control strategy based on a model which incorporates the principle parameters of the RO desalination processes has to be implemented. Thus, many research have been carried out to establish a suitable model based on relations between the inputs and the outputs variables of the plant. This paper deals with a new multivariable state-space nonlinear model that we have developed for the RO desalination system. The main contribution of this work is the use of appropriate physical equations of the reverse osmosis phenomenon to develop this dynamic model. The efficiency of the established model is demonstrated through computer dynamic simulation and validated by experimental results obtained by a real data acquisition interface coupled to a RO desalination prototype.

Keyword: Reverse osmosis, Desalination, Mathematical Model, Control, state-space model.

Nomenclature

$C^*_{p,b}$	thermal capacity average (kJ kg^{-1} K^{-1})
d_i	fiber intern diameter (m)
F_{bp}	loss of water between brine and permeate side (kg. h^{-1})
F_f	flow rate of feed water (kg. h^{-1})
F_m	flow rate in membrane side (kg. h^{-1})
C_b	concentration in brine side (kg. m^{-3})
L_b	brine tube length (m)
m_b	water mass in brine side (kg)

P_b	brine pressure (bar)
P_f	feed pressure (bar)
P_{max}	maximal pressure
$\dot{Q}_b$	heat (W)
T_b	brine temperature (K)
T_f	feed temperature (K)
$\Delta\pi^*$	osmotic pressure average (bar)
T_p	permeate temperature (K)
η_b	water viscosity (kg. m^{-1} .h^{-1})
ρ_b	Fluid density(kg.m^{-3})

1. Introduction

Reverse Osmosis desalination systems are the most widely used processes [1] to provide fresh water for drinking or irrigation especially in arid or semi-arid regions with high water salinity. Therefore, the intensive demand on water resources requires a lot of desalination installations making a huge quantity of electrical energy necessary [2]. To improve the plant efficiency and produce fresh water with high quality and low cost, optimum operating conditions using advanced control techniques are required [3]. In literature, several dynamic models have been developed in recent years. They can be classified into two types: The first types are based on input–output transfer models using different parameters. In the process described in [4], a dynamic matrix control algorithm based on the manipulation of the pH and the pressure was developed. However, this approach cannot be used in the case of an RO plant designed for brackish water where the salinity is lower than that of the sea water and the variation of pH is not significant. Chaabene et al. [5] have developed a multi-input multi-output transfer model based on experimental results for a small RO desalination system fed by a photovoltaic generator. This model reflects the real dynamic of the system but it does not present the physical parameters.

These types of models present several difficulties to be implemented in a control strategy due to either the choice of the input-output parameters or to the inexistence of physical relations between these parameters.

The second type of dynamic models presents the theoretical equations of the solution-diffusion phenomenon of the desalination using reverse osmosis [6,7, 8, 9, 10, 11]. In [12], a photovoltaic energy reverse osmosis system was proposed. Other predictive and periodic models [13,14] have also being used to control reverse osmosis desalination process.

Although, the importance of all these respected approaches, RO desalination systems models are limited by either the complexity of the model form or by the absence of certain system's parameters[15, 16, 17].

Journal of Engineering Technology
Volume 6, Issue 2, July. 2018, PP. 1-12
RESEARCH ARTICLE -ENGINEERNG TECHNOLOGY

A mathematical model taking into account physical expressions is essential to study the relations between the system parts and their suitability for control strategies.

The main contribution of this study will be to build a state-space model based on the physical laws of mass conservation and the chemical laws of solution-diffusion phenomenon. Furthermore, the present model will study the behavior of the two quality parameters, the water flow and salinity to a much higher accuracy requirement to represent the system dynamic adequately.

Using Mathlab Software the developed model was simulated to generate data about the dynamic behavior of the RO desalination system. An experimental plant is also tested; the experimental results are compared to the simulated ones in order to validate the dynamic model and the system working properties.

2. Reverse osmosis principle

The RO unit membrane (Fig.1) is the principal component of the system. It is a semi-permeable polyamide membrane, composed of two sides: a brine side and a permeate side. The brackish or sea-water is pumped into a closed vessel and pressurized by a High Pressure (HP) pump against the membrane where the salt solution is rejected by the brine side, but the desalted pure water passes through the permeate side.

Figure 1. Reverse osmosis principle

3. Composition and Physical models of the ROD system

As is shown in Figure 2, the system is composed of three compartments which are the brine side, the permeate side and the membrane side.

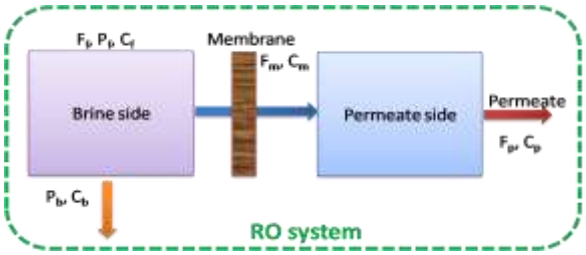

Figure 2. Compartments of the RO desalination system

The following expressions given in [18] present physical models based on the diffusion phenomenon. These relations show the conservation principles of the water flow, the pressure and the salt concentration for each side of the system.

3.1. Physical model of the brine side

The conservation principle of the parameters: feed pressure and salt concentration through the brine side gives Equations (1) and (2) [16]:

$$\frac{dC_b}{dt} = \frac{1}{m_b} \times [F_f \times (C_f - C_b) - F_m \times (C_p - C_b)] \quad (1)$$

$$\frac{dP_f}{dt} = \frac{1}{L_b} \times (P_b - P_f - \emptyset \times F_f) \quad (2)$$

With

$$L_b = \frac{32 \times \eta_b \times {l_b}^2}{{d_i}^2 \times P_{max}} \quad (3)$$

$$\emptyset = \frac{128 \times \eta_b \times l_b}{\pi \times \rho_b \times {d_i}^2} \quad (4)$$

3.2. Physical model of the permeate side

The conservation principle of the flow rate and the salt concentration through the permeate side gives Equations (5) and (6) [18]:

$$\frac{dm_p}{dt} = F_m - F_p \quad (5)$$

$$\frac{dC_p}{dt} = \frac{F_m \times (C_m - C_p)}{m_p} \quad (6)$$

3.3. Physical model of the membrane side

The flow rate in the membrane side is given by the following equation:

$$F_m = B_0 \times e^{b_T \times \frac{T_m - T_0}{T_m}} \times C_f + A_0 \times \rho_p \times e^{a_T \times \frac{T_m - T_0}{T_m}} \times (P_f - \Delta\pi^*) \quad (7)$$

The osmotic pressure average $\Delta\pi^*$ is proportional to the difference between the salt concentrations of the rejected water on the brine side and that of the permeate water:

$$\Delta\pi^* = k(C_b - C_p) \quad (8)$$

where k is a constant, $k=3.10^{-6}$ [18]:

Thus, from Equations (7) and (8), the expression of the flow rate in the membrane is expressed as follows:

$$F_m = A' \times P_f + B' \times C_f - A' \times \Delta\pi^* = A' \times P_f + B' \times C_f + A'' C_p - A'' C_b \quad (9)$$

with

Journal of Engineering Technology
Volume 6, Issue 2, July. 2018, PP. 1-12
RESEARCH ARTICLE -ENGINEERNG TECHNOLOGY

$$A' = A_0 \times \rho_p \times e^{a_T \times \frac{T_m - T_0}{T_m}} \quad (10)$$

$$B' = B_0 \times e^{b_T \times \frac{T_m - T_0}{T_m}} \quad (11)$$

$$A'' = kA' = 3.10^{-6} A' \quad (12)$$

Assumptions

Taking into account the experimental plants proprieties, some assumptions are given in order to simplify the model.

1. The flow is laminar
2. The reverse osmosis membrane is totally full of water;
3. The water masses in the brine side and the permeate side are constants so, $\frac{dm_p}{dt} = 0 \ \ and \ \frac{dm_b}{dt} = 0$
4.The salt concentration in the brine side is proportional to that in the brine side $C_m = \varepsilon C_b = 1.05. C_b$.

4. State space model of the RO Desalination system

4.1. Input -output parameters

The permeate water flow rate F_p and the permeate water concentration (or salinity) C_p are the two output quality parameters of the RO desalination system [19]. The brine pressure P_b and the feed water flow F_f are the input parameters. The water feed salinity C_f, considered as a disturbance, must be controlled to avoid membrane scaling. Figure 3 shows the input- output static model of the RO desalination system.

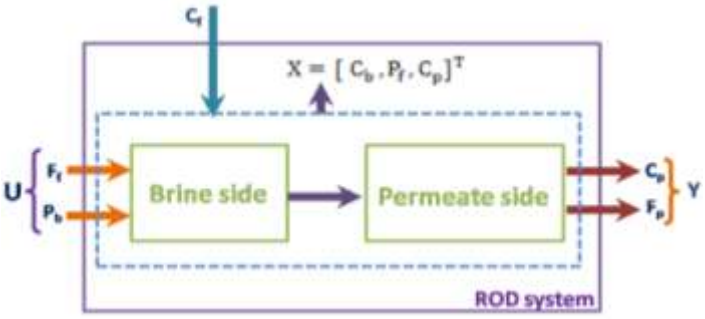

Figure 3. Static Input Output model of the RO desalination system

4.2. State space model of the RO Desalination system

The typical state space model [19] of the system is given by Equation (13):

$$\dot{X} = AX + BU$$

$$\text{With } X = [C_b, P_f, C_p]^T \text{and } U = [F_f, P_b]^T \quad (13)$$

If we replace all the parameters by their expressions from Equation (1), (2) and (6), the state-space model

of the RO desalination system can be given by Equation (14):

$$\begin{bmatrix}\dot{C}_b\\ \dot{P}_f\\ \dot{C}_p\end{bmatrix}=\begin{bmatrix}\frac{F_m-F_f}{m_b} & 0 & -\frac{F_m}{m_b}\\ 0 & -\frac{1}{L_b} & 0\\ \varepsilon\frac{F_m}{m_P} & 0 & -\frac{F_m}{m_P}\end{bmatrix}\begin{bmatrix}C_b\\ P_f\\ C_p\end{bmatrix}+\begin{bmatrix}\frac{C_f}{m_b} & 0\\ -\frac{\emptyset}{L_b} & \frac{1}{L_b}\\ 0 & 0\end{bmatrix}\begin{bmatrix}F_f\\ P_b\end{bmatrix} \quad (14)$$

The expression of the system outputs is represented by Equation (15):

$$Y=CX+Z \qquad \text{With} \qquad Y=\begin{bmatrix}F_p\\ C_p\end{bmatrix} \quad (15)$$

Taking into account assumption (3):

$$\frac{dm_p}{dt}=F_m-F_p=0 \quad than \quad Fm=Fp \quad (16)$$

From Equations (9) and (16), the outputs state space expression is given by Equation (17):

$$\begin{bmatrix}F_p\\ C_p\end{bmatrix}=\begin{bmatrix}-A'' & A' & A''\\ 0 & 0 & 1\end{bmatrix}\begin{bmatrix}C_b\\ P_f\\ C_p\end{bmatrix}+\begin{bmatrix}B'\times C_f\\ 0\end{bmatrix} \quad (17)$$

Finally, the global state-space model of the RO desalination system can be represented by Equation (18):

$$\begin{cases}\begin{bmatrix}\dot{C}_b\\ \dot{P}_f\\ \dot{C}_p\end{bmatrix}=\begin{bmatrix}\frac{F_m-F_f}{m_b} & 0 & -\frac{F_m}{m_b}\\ 0 & -\frac{1}{L_b} & 0\\ \varepsilon\frac{F_m}{m_P} & 0 & -\frac{F_m}{m_P}\end{bmatrix}\begin{bmatrix}C_b\\ P_f\\ C_p\end{bmatrix}+\begin{bmatrix}\frac{C_f}{m_b} & 0\\ -\frac{\emptyset}{L_b} & \frac{1}{L_b}\\ 0 & 0\end{bmatrix}\begin{bmatrix}F_f\\ P_b\end{bmatrix}\\ \begin{bmatrix}F_p\\ C_p\end{bmatrix}=\begin{bmatrix}-A'' & A' & A''\\ 0 & 0 & 1\end{bmatrix}\begin{bmatrix}C_b\\ P_f\\ C_p\end{bmatrix}+\begin{bmatrix}B'\times C_f\\ 0\end{bmatrix}\end{cases} \quad (18)$$

As the flow rate F_m depends on the state-space arrow X, the state-space equation can be represented by Equation (19):

$$\begin{cases}\dot{X}=A(x)X+BU\\ Y=CX+Z\end{cases} \quad (19)$$

4.3.Linearization of the state-space equation

The state-space equation can be written as $\dot{X} = f(X,U)$ with:

$X = [\,C_b, P_f, C_p]^T = [x_1, x_2, x_3]^T$ and $U = [\,F_f, P_b\,]^T = [\,u_1, u_2\,]^T$ so we obtain the Equation (20):

$$\begin{cases} f_1(x,u) = \dfrac{F_m - F_f}{m_b} x_1 - \dfrac{F_m}{m_b} x_3 + \dfrac{C_f}{m_b} u_1 \\ f_2(x,u) = -\dfrac{1}{L_b} x_2 - \dfrac{\phi}{L_b} u_1 + \dfrac{1}{L_b} u_2 \\ f_3(x,u) = \dfrac{F_m}{m_p}(\varepsilon x_1 - x_3) \end{cases} \quad (20)$$

Around the working point, the two state-space matrices are defined as follows:

$$A = \left[\begin{matrix} \frac{\partial f_1}{\partial x_1} & \frac{\partial f_1}{\partial x_2} & \frac{\partial f_1}{\partial x_3} \\ \frac{\partial f_2}{\partial x_1} & \frac{\partial f_2}{\partial x_2} & \frac{\partial f_2}{\partial x_3} \\ \frac{\partial f_3}{\partial x_1} & \frac{\partial f_3}{\partial x_2} & \frac{\partial f_3}{\partial x_3} \end{matrix}\right]_{\vec{x},\vec{u}} \qquad B = \left[\begin{matrix} \frac{\partial f_1}{\partial u_1} & \frac{\partial f_1}{\partial u_2} \\ \frac{\partial f_2}{\partial u_1} & \frac{\partial f_2}{\partial u_2} \\ \frac{\partial f_3}{\partial u_1} & \frac{\partial f_3}{\partial u_2} \end{matrix}\right]_{\vec{x},\vec{u}} \quad (21)$$

According to Equation (9), the flow rate in the membrane depends on the system's inputs and outputs. So, it can be written as $F_m = f(X,U)$. Consequently, the components of the two matrices are determined by Equations (22), (23) and (24):

$$\begin{cases} \dfrac{\partial f_1}{\partial x_1} = \dfrac{1}{m_b}(-2\varepsilon A'' x_1 + (1+\varepsilon)A'' x_3 + A' x_2 + (B' C_f - u_1)) \\ \dfrac{\partial f_1}{\partial x_2} = \dfrac{A'}{m_b}(x_1 - x_3) \\ \dfrac{\partial f_1}{\partial x_3} = \dfrac{1}{m_b}(A''((1+\varepsilon)x_1 - 2x_3) - B' C_f) \\ \dfrac{\partial f_1}{\partial u_1} = \dfrac{1}{m_b}(-x_1 + C_f) \\ \dfrac{\partial f_1}{\partial u_2} = 0 \end{cases} \quad (22)$$

$$\begin{cases} \dfrac{\partial f_2}{\partial x_1} = 0 \\ \dfrac{\partial f_2}{\partial x_2} = -\dfrac{1}{L_b} \\ \dfrac{\partial f_2}{\partial x_3} = 0 \\ \dfrac{\partial f_2}{\partial u_1} = -\dfrac{\phi}{L_b} \\ \dfrac{\partial f_2}{\partial u_2} = \dfrac{1}{L_b} \end{cases} \quad (23)$$

$$\begin{cases} \dfrac{\partial f_3}{\partial x_1} = \dfrac{1}{m_p}(\varepsilon A' x_2 + A''(1+\varepsilon)x_3 - 2\varepsilon^2 A'' \varepsilon x_1 + \varepsilon B' C_f) \\ \dfrac{\partial f_3}{\partial x_2} = \dfrac{A'}{m_p}(\varepsilon x_1 - x_3) \\ \dfrac{\partial f_3}{\partial x_3} = \dfrac{1}{m_p}(-A' x_2 + A''(1+\varepsilon)x_1 - B' C_f - 2A'' x_3) \\ \dfrac{\partial f_3}{\partial u_1} = 0 \\ \dfrac{\partial f_3}{\partial u_2} = 0 \end{cases} \quad (24)$$

5. Results and discussion

In order to check the dynamic behavior of the RO desalination system model, computer simulation based on Mathlab Simulink software can be carried out by adopting the applicable values for the parameters of the model around a working point. Furthermore, in order to validate the established dynamic model, a RO desalination plant equipped with a real data acquisition system is used in experimental tests [20,21]. The simulated results are then compared with the experimental ones.

If we replace the parameters in Equations (22), (23) and (24) by their values, the numerical parameters of the state-space model are determined as follows:

$$A = \begin{bmatrix} -102.6 & 0 & -2403.5 \\ 0 & -10 & 0 \\ 4.6 & 0 & -1538.3 \end{bmatrix}_{\bar{x},\bar{u}} \quad B = \begin{bmatrix} 43.856 & 0 \\ 0.005 & 10 \\ 0 & 0 \end{bmatrix}_{\bar{x},\bar{u}} \quad (25)$$

$$C = \begin{bmatrix} 0.05 & 57.9 & 0.05 \\ 0 & 0 & 1 \end{bmatrix}_{\bar{x},\bar{u}} \quad D = 0 \quad Z = \begin{bmatrix} 67.137 \\ 0 \end{bmatrix}_{\bar{x},\bar{u}}$$

Journal of Engineering Technology
Volume 6, Issue 2, July. 2018, PP. 1-12
RESEARCH ARTICLE -ENGINEERNG TECHNOLOGY

5.1. Analysis of Simulation results

Figure 4 represents the behavior of the salt concentration of the permeate water C_p and the permeate water flow F_p for different feed water salinities C_f.

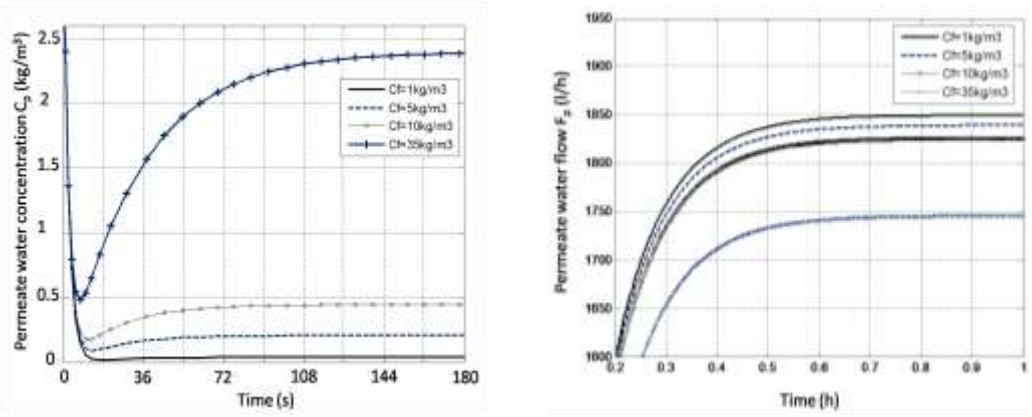

Figure 4. Simulated results of the permeate water concentration and flow with different feed water salinities

The increasing of the permeate water salinity with the feed water salinity is justified by the increasing of the salt flow Q_s through the membrane as it is proportional to the feed water salinity according to its expression given by Equation (26) [7]:

$$Q_s = k(C_f - C_p) \quad (26)$$

According to Equations (7) and (8), when the feed water salinity increases, the osmotic pressure average $\Delta\pi^*$ increases, thus, the permeate flow rate decreases. This result can be clearly observed in Fig.4, where the permeate water flow decreases from 1850 kg/h for a feed water salinity of 1kg/m^3 to 1750 kg/h for the maximum salinity of 35kg/m^3 .

5.2. Experimental results

Figure5 shows the setup of the RO desalination experimental platform installed in the Research and Technology Center of Energy at the Technology Park of Borj-Cedria, Hammam-Lif, Tunisia. As it is shown, the system is composed of a feed water pump, three reverse osmosis modules containing the membranes and a data acquisition system equipped with sensors to measure the flow rate, the salinity and the pressure.

Journal of Engineering Technology
Volume 6, Issue 2, July. 2018, PP. 1-12
RESEARCH ARTICLE -ENGINEERNG TECHNOLOGY

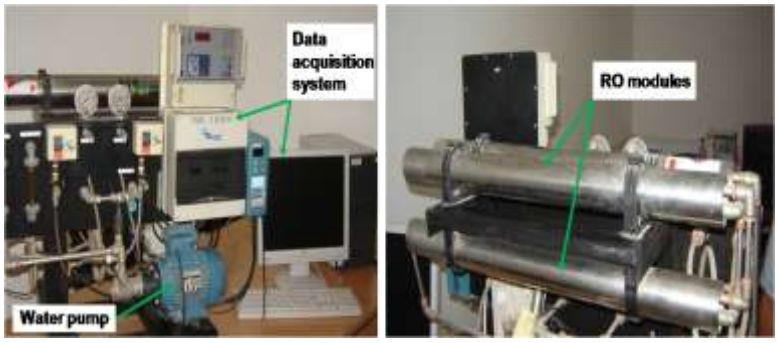

Figure 5. The RO Desalination experimental set up

A comparison of the experimental and simulated evolution of the product water salinity C_p and the permeate water flow rate was given in figure 6. As it is shown, the simulated curve lags slightly behind the experimental curve. The curves show significant correlation between the dynamic behavior of the RO Desalination system and its developed state-space model. Furthermore, the comparison between Figure 4 and Figure 6 shows that curves have the same evolution.

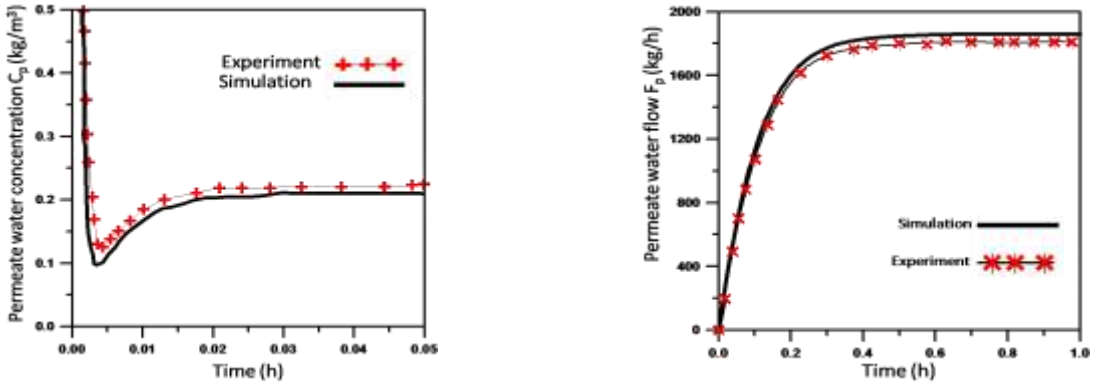

Figure 6. Model validation of the permeate water concentration C_p

As we have used brackish water in experimental tests, it can be found that the maximum value can be different depending on the used feed water salinity which can affect the initial or final values without any influence on the curve-form. Thus, the dynamic behavior of the system and its model is the same.

6. Conclusions

In this article, a new dynamic model of the Reverse Osmosis Desalination system is proposed. The established model is developed after decomposition of the system into subsystems. By the use of physical equations and the coupling of sub models of the brine side and the permeate side, a multivariable state-space model was developed. Subsequently, the proposed model was simulated and a small RO desalination system is tested to validate the dynamic model. It has been shown that there is a significant correlation between the experimental and simulated results. The selected input-output parameters reflect

the permeate water quality and it is becoming increasingly important to operate them as close as possible to target. By comparing the database of reference data with the obtained results, the solutions proposed by this model are innovative. Indeed, the mathematical form of the model simplifies its implementation on real systems and the relations between the different parameters are deduced from the physical equations of physic-chemical phenomena of the reverse osmosis desalination technique.
As a perspective of this work, design and implementation of control strategy based on the developed model will be carried out to operate the RO desalination system at optimum conditions.

References

[1] A.J. Dabbabneh, M.A. Al-Nimr, A reverse osmosis desalination unit, Desalination, 153(2002**)** 265-272.
[2] A.R. Bartman, A. Zhu, P.D. Christophidies, Y. Cohen, Minimizing energy consumption in reverse osmosis membrane desalination using optimization based control, Journal of Process Control, vol. 20, (2010) 1261-1269.
[3] I. Alatiqui, H. Ettouney, H. El-Dessouky, Process control in water desalination industry: an overview, Desalination, vol.126, (1999) 15-32.
[4] M.W. Robertson, J.C. Watter, P.B. Desphande, J.Z. Assef, I. Alatiqui, Model based control for reverse osmosis desalination process, Desalination, vol.104, (1996) 59-68.
[5] A. Ben Chaabene, R. Andolsi, A. Sellami, R. Mhiri, MIMO Modeling approach for a small photovoltaic reverse osmosis desalination system, Journal of Applied Fluid Mechanic vol.4, (2011**)** 35-41.
[6] B. Ballannec, S. Nicolas and B. Bariou, Experimental study and modeling of reverse osmosis with salt solutes in unstirred batch cell, Desalination, vol. 122 (1999), pp. 43-51.
[7] G.I.M. Worn, M. Van Der Wees, J.C.F. De Winter, L. De Graaf, P.A. Wieringa, L.C. Rietveld, Training and Assessment with a faster than real time simulation of a drinking treatment plant, Journal of Simulation Modeling Practice and Theory, vol. 21,(2012), pp. 52-64.
[8] A. Hossam-Eldine, A.M. El-Nashar, A. Isamail, Techno economic optimization of SWRO desalination using advanced control approach, Journal of Desalination and Water Treatment, vol. 12, (2009**),** pp**.** 389-399.
[9] N. Fraidenraich, O. C. Vilela, M. D. S. Viana, J. M. Gordon, Improved analytic modeling and experimental validation for brackish-water reverse-osmosis desalination, Desalination, vol. 380, (2016), pp. 60-65.
[10] A. Jogdand, A. Chaudhuri, Modeling of concentration polarization and permeate flux variation in a roto-dynamic reverse osmosis filtration system, Desalination, vol. 375, (2015), pp. 54-70.
[11] N. Fradenraich, O.C. Vilela, G.A. Lima, J.M. Gordon, Reverse osmosis desalination: modeling and experiment, Applied Physics Letters, vol.94, (2009), pp. 102-124.
[12] A. Colangelo, D. Marano, G. Spagna, V.K. Sharma, Photovoltaic powered reverse osmosis water desalination system, International Journal of Applied Energy, vol. 64, (1999), pp. 289-305.

[13] L.G. Palacin, F. Tadeo, H. Elfil, C. de Prada, J. Salazar, New dynamic library of reverse osmosis plants with fault simulation, Journal of Desalination and Water Treatment, vol. 25 (2011), pp. 127-132.
[14] A.R. Bartman, C.W. McFall, P.D. Christophidies, Y. Cohen, Model predictive control of feed flow reversal in a reverse osmosis desalination process, Journal of Process Control, vol. 19, (2009),pp. 433-442.
[15] A. Emad, A. ajbar, I. Almutaz, Peroidic control of a reverse osmosis desalination process, Journal of Process Control, vol. 22, (2012), pp. 218-227.
[16] C.W. McFall, P.D. Christofides, Y. Cohen, J.F. Davis, Fault-tolerant control of a reverse osmosis desalination process, in: Proceeding of 8th IFAC Symposium on Dynamics and Control of Process Systems, vol.3, Cancun, Mexico, 2007, pp. 163-168.
[17] B.D.H. Phuc, S.S. You, T.W. Lim, H.S. Kim, Dynamical analysis and control synthesis of RO desalination process against water hammering, Desalination, vol. 402, (2017), pp.133-142.
[18] A. Gambier, A. Krasnick, E. Badreddine, Dynamic modeling of a simple reverse osmosis desalination plant for advanced control purposes, Proceeding of the 2007 American Control Conference (2007), pp. 4814-4819.
[19] W. Favoreel, B. de Moor, P.V. Overshee, State space system identification for industrial processes, Journal of Process Control, vol. 10, (2000), pp. 149-155.
[20] A. Ben Chaabene, K. Ouelhazi, A. Sellami, Novel design and modeling of a photovoltaic hydro electromagnetic reverse osmosis (PV-HEMRO) desalination system, Journal of Desalination and Water Treatment, vol. 66, (2017), pp. 36-41.
[21] A. Ben Chaabene, K. Ouelhazi, A. Sellami, Following Control Of MIMO Uncertain Systems, Application to a Water Desalination System Supplied by Photovoltaic Source, Journal of Engineering Technology, vol.6, (2018), pp. 1-12.